JOURNAL OF CATALYSIS 37, 416–423 (1975)

Effect of the Pore Size on the Aging of Supported Metals

E. RUCKENSTEIN AND B. PULVERMACHER

Faculty of Engineering and Applied Sciences,
State University of New York at Buffalo,
Buffalo, New York 14214

Received August 6, 1974

The aging of supported metal crystallites is caused, under certain conditions, by the diffusion of the crystallites upon the surface of the substrate and by the sintering of the colliding particles. If the size of a crystallite is of the order of magnitude of the diameter of the pore, the diffusion of the crystallite will be impeded. A two-dimensional coagulation equation is formulated to describe the time dependence of the sizes of the population of crystallites into a porous substrate. Two models are used for the diffusion coefficient of the crystallites upon the substrate. In one of them, the diffusion coefficient is inversely proportional to the area of the interface between particle and substrate, even when diffusion is impeded. In the other, the diffusion coefficient is assumed to behave as in the first model for particle sizes smaller than the diameter of a pore but is taken to be zero when the sizes of the particle and pore become of the same order. On the basis of the proposed models information about the size distribution and the decay of the exposed surface area of the metal is obtained. A comparison between the unimpeded diffusion on a planar substrate and the impeded diffusion inside a porous substrate is presented.

NOMENCLATURE

c_k	concentration per unit surface area of substrate of crystallites composed of k units
d_{av}	$(\phi/N)^{1/3}$, average particle diameter obtained from magnetic measurements
d_{vs}	$d_{vs} = 5/\rho\bar{S}$, chemisorption diameter of the crystallites
D_i	diffusion coefficient of a crystallite composed of i units
$D_{ij} \equiv$	$D_i + D_j$
$f(t)$	random force
i_p	L_p^3/v_1
k	Boltzman constant; also subscript indicating the number of atoms of metals
$K(v,\tilde{v})$	collision frequency factor in the continuous representation
K_{ij}	collision frequency factor in the discrete representation
K^*	$4\pi/\ln 4T$
L_i	dimension of the crystallite composed of i units
L_p	diameter of the pore
m	mass of a crystallite
$n(v,t)$	density distribution of sizes
N	total number of crystallites per unit surface area of support
N_0	value of N for $t = 0$
R_{ij}	radius of interaction between two colliding crystallites
R_G	Guiner radius
R_p	Porod radius
s_i	area of the interface between one crystallite and the substrate
S	exposed surface area of metal per unit surface area of support; S_0 = value of S at $t = 0$
$\bar{S}$	exposed surface area of metal per gram of metal
t	time
T	$D_{ij}\theta^*/(R_{ij})^2 \approx D_{11}\theta^*/(R_{11})^2$; in

the evaluation of T, θ^* is taken as 1 sec; in Eq. (4) T is the temperature in °K

$\bar{u}$ velocity of the crystallite on the substrate

v volume of a crystallite

v_i volume of a crystallite composed of i units

δ delta function

ρ density of metal

ϕ total volume of particles per unit surface area of support

ψ^* dimensionless variable in the similarity representation [defined by Eq. (9a)]

μ surface friction coefficient [Eq. (4)]

η^* dimensionless variable in the similarity representation [defined by Eq. (9b)]

τ $K^*D_1N_0t$

INTRODUCTION

There is experimental evidence which demonstrates that small crystallites on a substrate migrate more or less randomly. For instance, Bassett (*1,2*), using an electron microscope, observed translation and rotation of copper and silver islands on a molybdenite substrate at a temperature of 525°K, and Skofronick and Phillips (*3*) and Phillips *et al.* (*4*) observed migration and coalescence of gold islands on amorphous carbon and silicon substrates at temperatures between 500 and 700°K. These observations, together with many other similar observations (*5–8*), have suggested representing the aging kinetics of the supported metal catalysts by a model accounting for diffusion of the crystallites on the substrate and sintering of the colliding particles (*9,10*). A two-dimensional coagulation equation was formulated to describe the time dependence of the sizes of the population of crystallites. In the models, it is assumed that particles migrate and grow upon a planar substrate. In supported metal crystallites the substrate has, however, a porous structure and it is natural to enquire about the effect the pore size distribution has upon the migration of crystallites inside the pores and, consequently, upon the aging process. The goal of the present paper is to provide some insight into this problem.

MODELS

The Physical Model

Many of the porous solids used as substrates show a bimodal pore size distribution because they are generally prepared by compacting fine porous powders. The resulting large particles have relatively large pores (macropores) consisting of spaces between the powder particles and small pores (micropores) within the powder particles themselves. For instance, the boehmite pellets prepared by Otani *et al.* (*11*) have a bidisperse distribution with a maximum of about 20 Å for the micropores and, depending upon the compacting pressure, a maximum size macropore varying from 500 to 5000 Å. The alumina substrate prepared by Rothfeld (*12*) had two peaks, one at 120 Å and another at 12,500 Å, and that prepared by Rao and Smith (*13*) had peaks at 30 and 1000 Å, respectively. For reviews, see Refs. [*14,15*]. In the majority of the cases the surface area of the macropores is only a few percent of the total surface area.

Because the surface area of the macropores is small compared to that of the micropores, the population of crystallites in the macropores will be neglected. Also, for the sake of simplicity, instead of considering a size distribution of the micropores, it will be assumed that the dispersion of sizes around the peak is small and consequently that the density distribution of pore sizes around the peak can be replaced by a δ function.

The number of crystallites, per unit surface area of substrate, composed of k

metal units satisfies the population balance (*9,10*),

$$\frac{dc_k}{dt} = \frac{1}{2}\sum_{i+j=k} K_{ij}c_ic_j - c_k\sum_{i=1}^{\infty} K_{ik}c_i, \qquad (1)$$

where K_{ij} are second order rate constants dependent upon the mobility of the crystallites upon the substrate and upon the rate of coalescence of colliding crystallites. The continuous version of the population balance has the form

$$\frac{\partial n}{\partial t} = \frac{1}{2}\int_0^v K(\tilde{v},v-\tilde{v})n(\tilde{v},t)n(v-\tilde{v},t)d\tilde{v} - n(v,t)\times\int_0^\infty K(\tilde{v},v)n(\tilde{v},t)d\tilde{v}, \qquad (1a)$$

where $n(v,t)dv$ represents the number of crystallites having a size between v and $v+dv$. Assuming that the coalescence process is rapid, the rate of aging is diffusion controlled and (*9,10*):

$$K_{ij} = K^*\,(D_i + D_j), \qquad (2)$$

where K^* is practically a constant.

The size of the pores influences the aging process via the diffusion coefficient D_i. To establish a relation between the diffusion coefficient, D_i, and the pore size, some comments concerning the diffusion process are in order. The starting point is the experimental observation that under certain conditions a crystallite migrates as a single entity upon the surface of the substrate. This migration probably is due to the random collisions produced by the oscillations of the atoms at the crystallite–substrate interface. If so, the theory of Brownian motion can be extended to the present situation. The theory of Brownian motion is based upon an equation of motion (the Langevin equation) (*16*) in which the effect of the surrounding medium on the motion of a particle is split into a systematic part and a fluctuating part. The systematic part represents the dynamical friction experienced by the particle, and the fluctuating part is caused by the random collisions. If one assumes that the resistance force is proportional to the velocity of the particle and to the interfacial area of the substrate–crystallite, Langevin's equation becomes

$$m\frac{d\bar{u}}{dt} = -\mu s\bar{u} + f(t). \qquad (3)$$

Using the technique familiar in the theory of the Brownian motion (*5,16*) one obtains

$$D_i = 2kT/\mu s_i. \qquad (4)$$

Two models are used here. In both, Eq. (4) plays an important part. In the first model, the diffusion coefficient is assumed to be inversely proportional to s_i, whereas in the second, the diffusion coefficient is assumed to be inversely proportional to s_i when the size of the crystallite is small and zero when the size becomes as large as that of the pore. In the first model, if the crystallite is small and of almost cubic shape, s_i is proportional to the square of the diameter L_i of the crystallite. If the crystallite is large enough to fill up the pore as a small prism, $s_i \propto v_i/L_p$. Although there are intermediary situations in which crystallites do not completely fill the pore, only the two mentioned limiting behaviors will be taken into account. Hence, for this case

$$D_i \propto v_i^{-2/3} \qquad \text{when } i \leqslant i_p \equiv \frac{L_p^3}{v_1}, \qquad (5a)$$

and

$$D_i \propto \frac{L_p}{4v_i} \qquad \text{when } i > i_p \equiv \frac{L_p^3}{v_1}. \qquad (5b)$$

The proportionality constant is assumed to be the same in both equations. In the second model

$$D_i \propto \frac{1}{L_i^2} \equiv v_i^{-2/3} \qquad \text{when } i \leqslant i_p, \qquad (6a)$$

and

$$D_i = 0 \qquad \text{when } i > i_p. \qquad (6b)$$

The First Model

The equations for the discrete spectrum were solved numerically for two initial size distributions: a log normal and a unisized distribution. A fourth-order Runge-Kutta method was used and as many equations (up to 1200) considered as were needed to ensure that no particle was lost in the calculations. In Figs. 1 to 4, some of the results are plotted and compared to the case of a planar substrate. In Fig. 1 the initial distribution is a log normal one, the size of the smallest particle is 20 Å and that of the pore 100 Å. Compared to the planar case, in this particular situation, there is no essential effect of the finite pore size on the size distribution. For the same situation, Fig. 2 shows that the finite size of the pore has an effect on the exposed surface area. The exposed surface area S is evaluated assuming crystallites of almost cubic shape with five exposed faces when they are small enough and of almost prismatic shape with two exposed faces when they fill the cross section of the pore. The intermediary range of particle shapes is

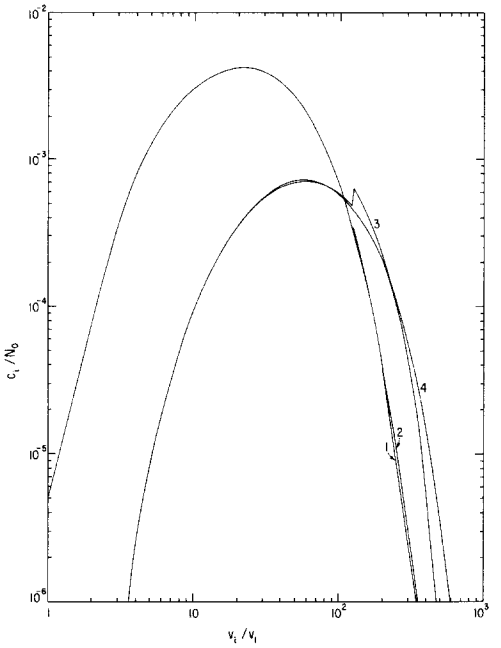

FIG. 1. Size distribution of crystallites. Size of the pores = 100 Å; the size of the smallest particle 20 Å log normal initial distribution

$$\frac{n(r)}{N} = \frac{1}{(2\pi)^{1/2} r \ln \sigma} \exp - \left(\frac{\ln r - \ln \mu}{2^{1/2} \ln \sigma}\right)^2,$$

where $\ln\mu = \ln R_G - 1.714 \ln (R_G/R_p)$ and $\ln^2\sigma = 0.286 \ln (R_G/R_p)$; $R_G = 29.5$ Å and $R_p = 20.5$ Å. (1) $\tau = 20$, $D_i \propto v_i^{-2/3}$ for $i \leqslant i_p$ and $D_i \propto v_i^{-1}$ for $i > i_p$; (2) $\tau = 20$, $D_i \propto v_i^{-2/3}$ (unimpeded diffusion); (3) $\tau = 100$, D_i as for Curve 1; (4) $\tau = 100$, D_i as for Curve 2.

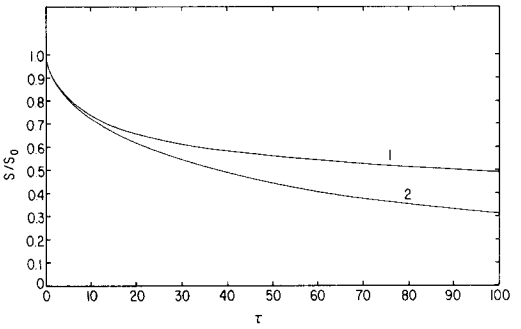

FIG. 2. The decay of the exposed surface area. The conditions are as for Fig. 1. (1) $D_i \propto v_i^{-2/3}$ (unimpeded diffusion); (2) $D_i \propto v_i^{-2/3}$ for $i \leqslant i_p$ and $D_i \propto v_i^{-1}$ for $i > i_p$.

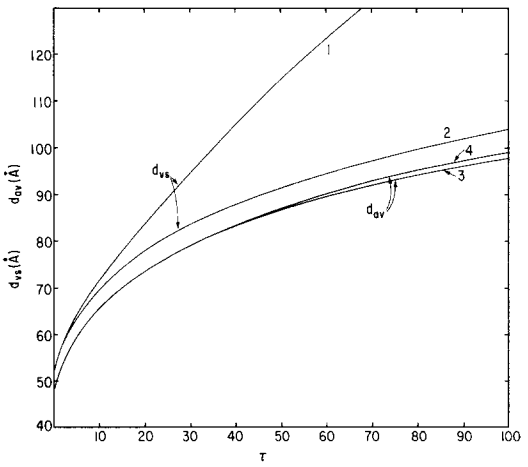

FIG. 3. Average particle size vs time. The conditions are as for Fig. 1. d_{vs} — average particle diameter obtained from chemisorption area $\equiv 5/\rho\bar{S}$; $d_{av} = (\phi/N)^{1/3}$ (high field magnetic radius). (1) d_{vs} for $D_i \propto v_i^{-2/3}$ for $i \leqslant i_p$ and $D_i \propto v_i^{-1}$ for $i > i_p$; (2) d_{vs} for $D_i \propto v_i^{-2/3}$ (unimpeded diffusion); (3) d_{av} (D_i as for Curve 1); (4) d_{av} (D_i as for Curve 2).

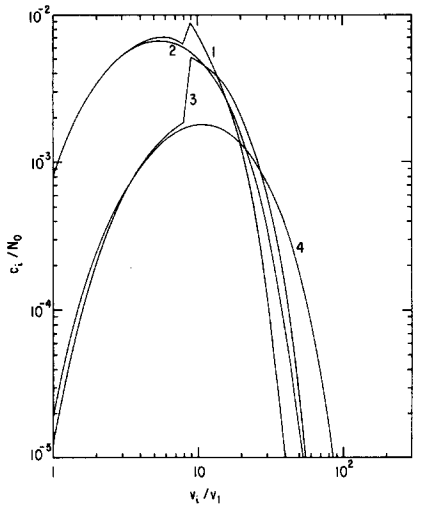

FIG. 4. Size distribution of crystallites. Size of the pores 100 Å; the size of the smallest particle, 50 Å. Unisized initial distribution. (1) $\tau = 25$, $D_i \propto v_i^{-2/3}$ for $i \leq i_p$ and $D_i \propto v_i^{-1}$ for $i > i_p$; (2) $\tau = 25$, $D_i \propto v_i^{-2/3}$ (unimpeded diffusion); (3) $\tau = 75$, D_i as for Curve 1; (4) $\tau = 75$, D_i as for Curve 2.

neglected. Consequently

$$S = \sum_{i=1}^{i_p} c_i 5 v_i^{2/3} + \sum_{i=i_p+1}^{\infty} 2 c_i L_p^2, \qquad (7)$$

where

$$i_p = \frac{L_p^3}{v_1}. \qquad (8)$$

The volume distribution of the crystallites in the pores is practically as for a planar substrate, whereas the decay of the exposed surface area of metal is different. This is due to the fact that as soon as the particles fill the cross section of the pore they have two faces of constant area exposed whereas because they grow, the size distribution continues to change.

For the same situation, in Fig. 3 two different average diameters are plotted vs the dimensionless time, τ, both for a planar and porous substrate. As expected, the chemisorption diameter, $d_{vs} = 5/\rho\bar{S}$, computed from the chemisorption area is much more sensitive to the finite pore size than the average diameter, $d_{av} = (\phi/N)^{1/3}$. Figure 4 shows that if the ratio between the size of the crystallites and the pore size becomes larger, the effect of the size of the pore on the volume distribution of crystallites is more important.

It was shown in a previous paper that, if the diffusion coefficient has an expression of the form (5a) over the complete range of sizes, then the size spectrum can be represented after a short time by a single curve in the coordinates

$$\psi^* = \frac{c_i \phi}{N^2 v_1} \qquad (9a)$$

and

$$\eta^* = \frac{N v_i}{\phi}. \qquad (9b)$$

The same coordinates are also useful when Eq. (5b) is used over the complete range of sizes. Of course, a different single curve is

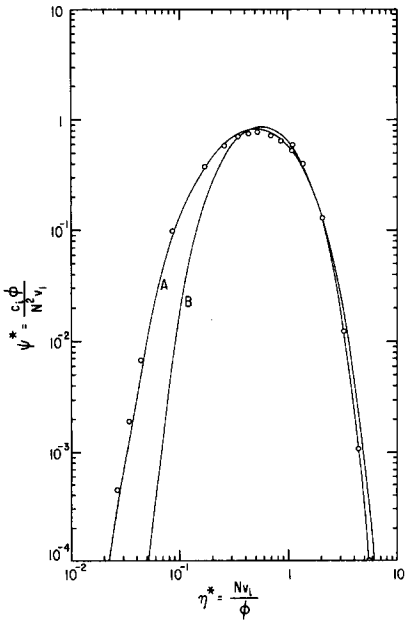

FIG. 5. Representation of the size spectrum in the similarity variables. Initially unisized distribution, cubes of 50 Å side, pores of 100 Å. (A) The similarity solution when $D_i \propto v_i^{-2/3}$; (B) the similarity solution when $D_i \propto v_i^{-1}$; (○) numerical solution of the population balance for $\tau = 100$ when $D_i \propto v_i^{-2/3}$ for $i \leq i_p$ and $D_i \propto v_i^{-1}$ for $i > i_p$.

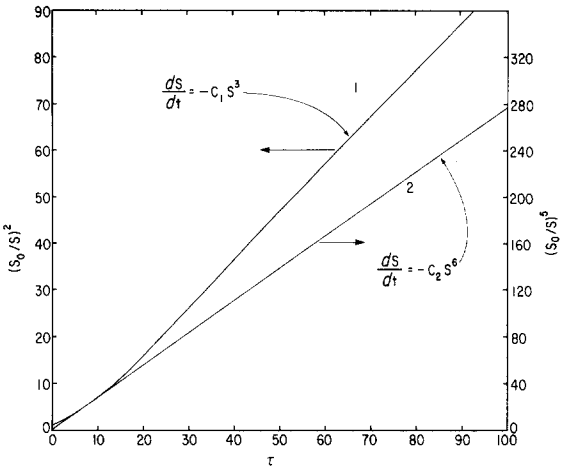

FIG. 6. Decay of the exposed surface area. Conditions are as for Fig. 4. (1) $D_i \propto v_i^{-2/3}$ $i \leq i_p$ and $D_i \propto v_i^{-1}$ $i > i_p$; (2) $D_i \propto v_i^{-2/3}$.

obtained in this case. Curve A in Fig. 5 is based on Eq. (5a) for the diffusion coefficient and Curve B is based on equation (5b). These curves have been obtained by numerically solving Eq. (1) for a unisized initial distribution. After a short time, the computed values become independent of the initial distribution and can be represented by a single curve in the coordinates (9a) and (9b). Figure 5 also shows that the points computed using (5a) for small particles and (5b) for large particles (the conditions are as for Fig. 4) superpose with Curve A for small sizes and with Curve B for larger sizes. Figure 6 shows that if the ratio between the size of the smallest crystallite and the size of the pore is large (for Fig. 6 it is 1/2) then the rate of decay is very different for the impeded diffusion and for diffusion on a planar substrate. After a sufficiently long time all the particles become large and, in the model used here, the exposed surface becomes proportional to the number of particles. In this limiting case one can show, on the basis of an equation established in (*10*), that

$$\frac{dN}{dt} \propto -N^3 \tag{10}$$

and consequently

$$\frac{dS}{dt} \propto -S^3. \tag{11}$$

For unimpeded diffusion it was shown in reference (*10*) that for a diffusion coefficient given by Eq. (5a)

$$\frac{dS}{dt} \propto -S^6. \tag{12}$$

Hence, if the diffusion of crystallites is strongly impeded, the exponent of S in the rate of decay of the exposed surface area of metal is decreased from six (for a planar substrate) to three.

The Second Model

Figure 7 shows the time evolution of the volume distribution. The discontinuities shown by the curves are due to the discontinuities in the value of the diffusion coefficient. For large enough times a steady state distribution is expected. Concerning the surface area, Fig. 8 shows that the two limiting cases give essentially the same results up to values of τ of the order of 70. For larger values, however, the exposed surface area obtained on the basis of the second model tends to a constant steady

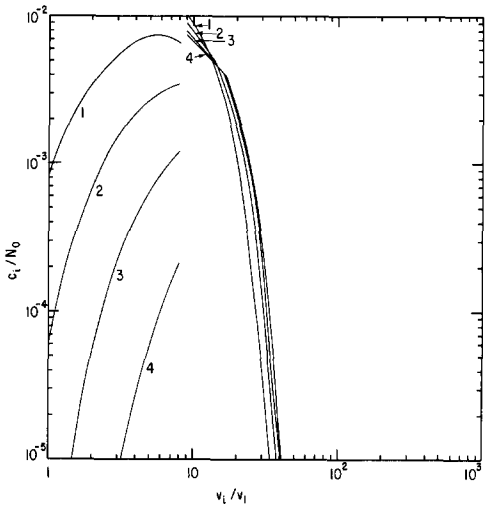

FIG. 7. Size distribution when $D_i \propto v_i^{-2/3}$ for $i \leq i_p$ and $D_i = 0$ for $i > i_p$. Unisized initial distribution, cubes of 50 Å side, pores of 100 Å. (1) $\tau = 25$; (2) $\tau = 50$; (3) $\tau = 100$; (4) $\tau = 200$.

state, while using the first model it is still decaying.

CONCLUSIONS

Two models are proposed to obtain some insight regarding the effect of pore size upon the aging of supported metals. In one of them it is assumed that the diffusion coefficient is inversely proportional to the area of the crystallite–substrate interface both when the equivalent diameter of the crystallites is smaller or larger than the diameter of the pore. In the other, the diffusion coefficient is also assumed inversely proportional to the area of the crystallite–substrate interface, but only until the equivalent diameter of the crystallite reaches the diameter of the pore. When the equivalent diameter of the crystallite is larger than the pore diameter, the diffusion coefficient is assumed zero.

Compared to the idealized planar substrate, the finite size of the pore has in the first model an effect when the ratio between the chemisorption diameter d_{vs} of the crystallites and the size of the pore is larger than about 1/2. For larger values of this ratio, the finite size of the pore has a stronger effect on the decay of the exposed surface area of metal than on the size distribution, and the exponent in the decay equation of the exposed surface area is decreased from six to three. In the second model a steady state distribution of sizes is achieved after a sufficiently long time. The decay of the exposed surface area of metal is practically the same for both models even for relatively long times. However, for very long times, the second model leads to a steady state value for the exposed surface area of the metal while the first model leads to a continuously decaying exposed surface area.

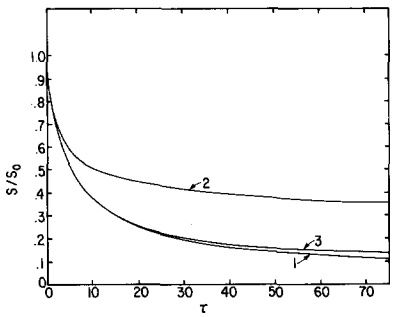

FIG. 8. Decay of the exposed surface area. Conditions as for Fig. 4. (1) $D_i \propto v_i^{-2/3}$ for $i \leq i_p$ and $D_i \propto v_i^{-1}$ for $i > i_p$; (2) $D_i \propto v_i^{-2/3}$ (unimpeded diffusion); (3) $D_i \propto v_i^{-2/3}$ for $i \leq i_p$ and $D_i = 0$ for $i > i_p$.

ACKNOWLEDGMENT

Acknowledgment is made to the donors of the Petroleum Research Fund, administered by the American Chemical Society, for support of this research.

REFERENCES

1. Basset, G. A., *in* "Proceedings of the European Regional Conference on Electron Microscopy" (A. L. Houwink and B. J. Spit, Eds.), Vol. 1. Delft, 1960.
2. Basset, G. A., *in* "Proceedings of the International Symposium on Condensation and Evaporation of Solids" (E. Rutner, R. Goldfinger and J. P. Hirth, Eds.). Gordon and Breach, New York, 1964.
3. Skofronick, J. G., and Phillips, W. B., *J. Appl. Phys.* **38**, 4791 (1967).

4. Phillips, W. B., Desloge, E. A., and Skofronick, J. G., *J. Appl. Phys*, **39**, 3210 (1968).
5. Kern, R., Mason, A., and Metois, J. J., *Surface Sci.* **27**, 483 (1971).
6. Metois, J. J., Gauch, M., Mason, A., and Kern, R., *Surface Sci.* **30**, 43 (1972).
7. Bachman, L., Sawyer, D. L., and Siegel, B. M., *J. Appl. Phys.* **36**, 304 (1965).
8. Reiss, H., *J. Appl. Phys.* **39**, 5046 (1968).
9. Ruckenstein, E., and Pulvermacher, B., *AIChE J.* **19**, 356 (1973).
10. Ruckenstein, E., and Pulvermacher, B., *J. Catal.* **29**, 224 (1973).
11. Otani, S., Wakao, N., and Smith, J. M., *AIChE J.* **11**, 439 (1965).
12. Rothfeld, L. B., *AIChE J.* **9**, 19 (1963).
13. Rao, M. R., and Smith, J. M., *AIChE J.* **11**, 485 (1963).
14. Wheeler, A., *in* "Advances in Catalysis" (W. G. Frankenburg, V. I. Komarewsky and E. K. Rideal, Eds.), Vol. 3, p. 249. Academic Press, New York, 1951.
15. Satterfield, C. N., "Mass Transfer in Heterogeneous Catalysis." M.I.T. Press, Cambridge, MA, 1969.
16. Chandrasekhar, S., *Rev. Mod. Phys.* **15**, 1 (1943).
17. Pulvermacher, B., and Ruckenstein, E., *J. Catal.* **35**, 115 (1974).